Optica Applicata, Vol. XXV, No. 4, 1995

Refractive properties of analytically approximated cornea

H. T. KASPRZAK

Institute of Physics, Technical University of Wrocław, Wybrzeże Wyspiańskiego 27, 50–370 Wrocław, Poland.

Refractive power of the cornea as approximated by conic curves and hyperbolic cosine profile is considered. Ray tracing technique is used for calculations of spot diagrams in different planes located in the focal region of the cornea. The light intensity distribution in each plane for different approximations and various diameters of the entrance pupil is calculated, depending on the local density of spots in the spot diagram. As a criterion of the light energy concentration in different planes of the focal region the polar moment of the second order I_{foc} of the light intensity distribution is evaluated. Curves presenting values of I_{foc} *vs.* position on the corneal axis for various corneal approximations are compared. It is shown that the highest concentration of the light energy is obtained in the case of elliptic approximations, then the medium one for the hyperbolic cosine profile and the lowest one for the hyperbola (case of keratoconus). The calculations prove that the form of distribution of I_{foc} for the reduced cornea with a single refractive surface and for the cornea with two approximated refractive surfaces is almost the same. The only difference is the shift of I_{foc} curves along the axis of the cornea.

1. Introduction

The cornea as a most refractive optical element of the eye contributes essentially to the quality of an image on the retina. Its refractive power amounts to about 70% of the refractive power of the whole eye. This is mainly due to the great difference between the refractive index of the air and an average refractive index of the cornea ($n_c = 1.3774$). This difference is about one order higher than the difference between an average refractive index of the crystalline lens and the refractive index of aqueous humor ($n_l = 1.39$, $n_a = 1.336$). Obviously the most important parameters of the cornea from the optical point of view are the corneal geometry and the average value of its refractive index. The corneal geometry is here understood as the topography of the external surface of the cornea and the distribution of the corneal thickness. It is well known that both corneal surfaces are aspheric [1], [2]. The asphericity of the anterior surface defined as the rate of changes of the radius of curvature is insignificant in its central part and increases towards the limbus. Both the topography of the external corneal surface and the variation of the corneal thickness constitute a very complex problem, playing an extremely important role in the modern ophthalmology.

Many authors studied the influence of the topography of the cornea on its refractive properties. MALONEY *et al.* [3] calculated differences between the corneal

topography measured by keratometry and the best-fit spherocylinder. CAMP *et al.* [4] calculated the influence of the corneal topography on the retinal image by use of the ray tracing method. SEILER *et al.* [5] used also the ray tracing technique to evaluate the longitudinal aberration of the cornea from the measured corneal topography.

Generally, the refractive properties of the cornea depend on the geometry and optical properties of consecutive layers of the cornea, starting from the tear film. Since 90% of the cornea is composed of stroma it is reasonable to neglect the influence of the other corneal layers and assume cornea to be optically homogeneous.

In order to calculate the refractive properties of the cornea its topography has to be described by use of more or less complex functions. WILSON and KLYCE [6] introduced the surface regularity index for the purpose of description of corneal topographic maps. For the sake of simplicity, the corneal topography can be approximated by some analytically expressed 3-D functions. In the case of corneas with a small axial astigmatism the rotationally symmetric corneal surface can be presented in a form of 2-D profile, being the axial section of the cornea.

There are many different analytical approximations of the corneal profile given in literature [1], [2], [7]. The conical curves [8]–[10], especially circle and an ellipse are the most frequently used curves for the approximation of the corneal profile. Sometimes the spherical approximation of both the corneal surfaces is used because of its simplicity and its reference to the commonly known refractive properties of spherical surfaces. However, as shown by KIELY *et al.* [8], the shape of the cornea assures significant (but not complete) reduction of its spherical aberration. This is why the elliptic approximation is often used. As it is well known from the geometrical optics, the rotationally symmetric ellipsoid has no spherical aberration in the case of parallel light beam illuminating the surface, only when the eccentricity of the ellipse is equal to the ratio of refractive indexes of media on both sides of the surface. Another simple approximation of the corneal contour which offers more "flexible" variations of its curvature is a hyperbolic cosine function [11]. Depending on the value of a parameter p, this profile enables not only monotonic variation of the radius of curvature as it is the case for conic curves but also non-monotonic changes as it is the case for some real corneas.

2. Method

The cornea was assumed to be a lens with the rotational symmetry. Both surfaces were approximated by circular, elliptic, hyperbolic, parabolic and hyperbolic cosine profiles, each described with one or two parameters. The refractive properties of the corneal model were calculated using ray tracing method for different diameters of the entrance pupil. The light intensity distribution was calculated as a local density of rays in the spot diagram, in different planes of the focal region, perpendicular to the optical axis of the model. The illuminating beam was assumed to be homogeneous and parallel. To assure the homogeneity of the illuminating beam, input rays were

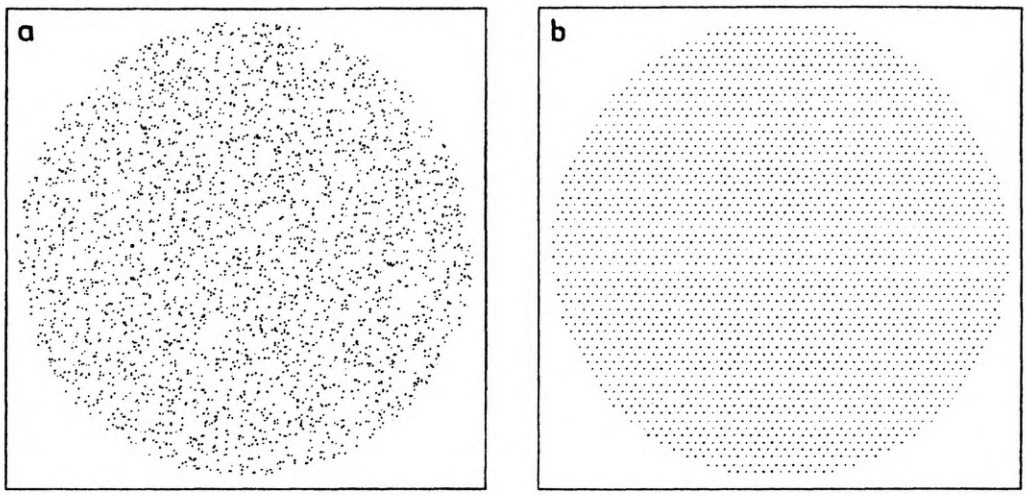

Fig. 1. Spot diagram of rays at the entrance pupil of the modeled cornea: **a** — random distribution **b** — ordering in triangles

distributed randomly or ordered in triangles (most dense packing) as shown in Fig. 1. Calculations showed that for 5000 rays or more the appropriate intensity distribution practically does not depend on the distribution of rays, whether random or ordered in triangles. Thus, in further computations only the randomly distributed rays hve been taken into account.

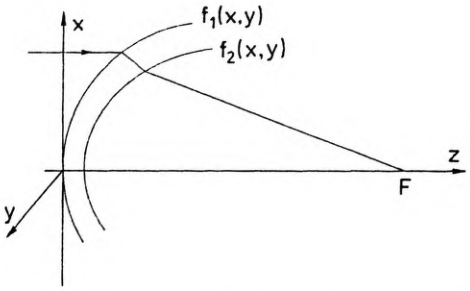

Fig. 2. Scheme of ray passing through the corneal model

The cornea was modeled both as a lens with varying thickness or as a single refractive surface (infinitely thin cornea). Figure 2 presents the section of the corneal model. The average refractive indexes of the cornea and the aqueous humor were assumed: $n_c = 1.3771$ and $n_a = 1.3374$, respectively. The spot density in the focal region was calculated in planes, located between the paraxial focus F_p and the focus of external rays F_e of the beam, as given in Fig. 3.

In the case of conic approximation, the external surface can be described by

$$z_1(x,y) = \frac{1}{\varepsilon_1^2 - 1}\left[\sqrt{R_{01}^2 + (x^2+y^2)(\varepsilon_1^2-1)} - R_{01}\right] \tag{1}$$

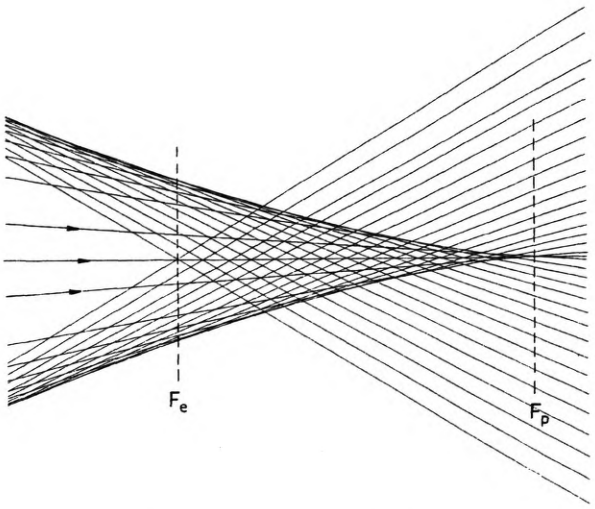

Fig. 3. Focal area of the corneal model. F_p – focus of paraxial rays, F_e – focus of external rays

where: R_{01} – central radius of curvature, ε_1 – eccentricity ($\varepsilon = 0$ for a circle, $0 < \varepsilon < 1$ for ellipse, $\varepsilon = 1$ for parabola and $\varepsilon > 1$ for hyperbola).

The inner surface was given in the form

$$z_2(x,y) = \frac{1}{\varepsilon_2^2 - 1}\left[\sqrt{R_{02}^2 + (x^2+y^2)(\varepsilon_2^2-1)} - R_{03}\right] + d \tag{2}$$

where: R_{02} – central radius of curvature, ε_2 – eccentricity, d – central thickness.

For the hyperbolic cosine approximation [11] both surfaces were given as

$$z_1(x,y) = \frac{R_{01}}{3p_1^2}\left[\cosh\left(\frac{\sqrt{3}p_1}{R_{01}}\sqrt{x^2+y^2}\right) - 1\right] \tag{3}$$

for the external surface, and

$$z_2(x,y) = \frac{R_{02}}{3p_2^2}\left[\cosh\left(\frac{\sqrt{3}p_2}{R_{02}}\sqrt{x^2+y^2}\right) - 1\right] \tag{4}$$

for the inner one.

For all approximations the central radii of the corneal curvature were assumed to be $R_{01} = 7.8$ mm and $R_{02} = 6.5$ mm, and the central thickness of the cornea $d = 0.52$ mm. Figure 4 presents examples of spot diagrams of the spherically approximated cornea, for the diameter of the entrance pupil $\varphi = 2$ mm. The presented spot diagrams were calculated for 3000 rays in three different planes of the focal region of the cornea. The respective 3-D distributions of the light intensity shown in Fig. 5 were calculated from spot diagrams of 5000 rays by angular averaging. In order to differentiate the concentration of the light energy around the optical axis in the focal region, a polar moment of the second order of the obtained light intensity

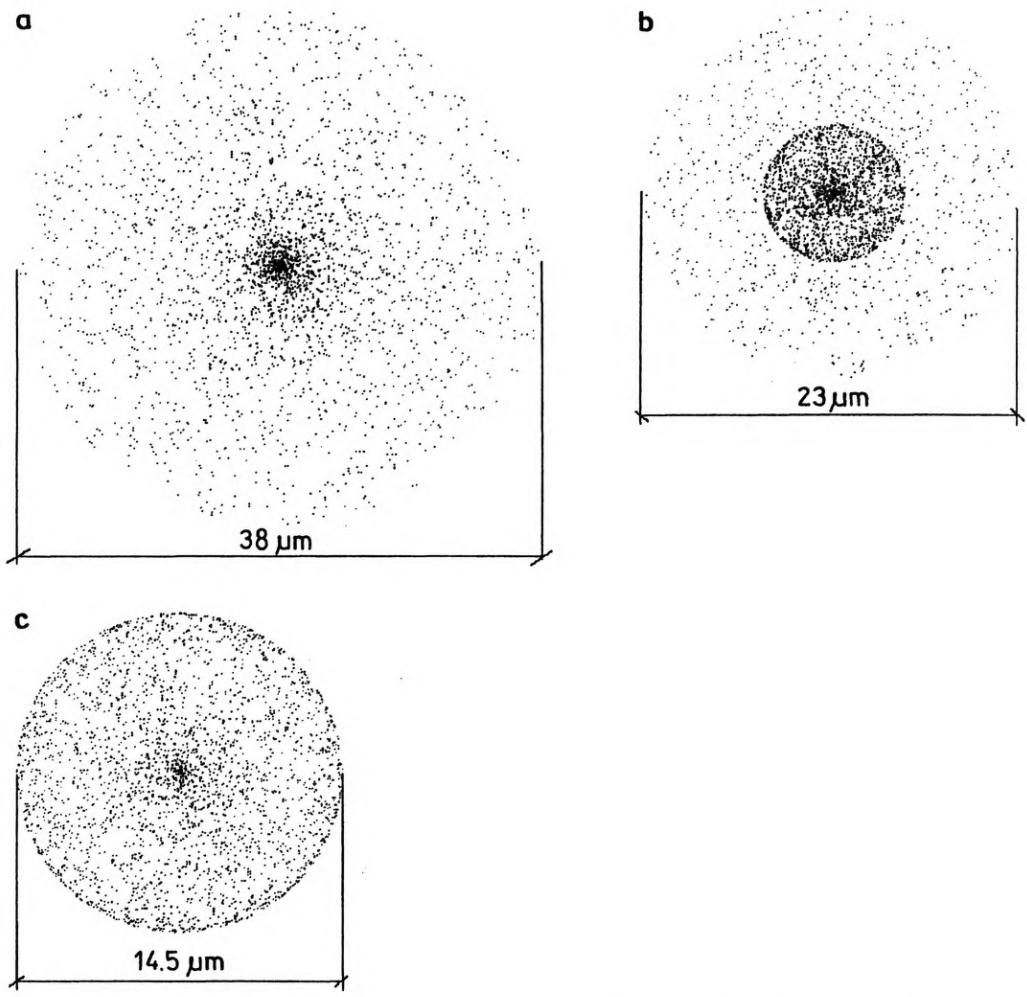

Fig. 4. Examples of spot diagrams of the cornea, approximated by means of two spheres in its focal region, calculated for 3000 rays: **a** — in the plane of the paraxial focus F_p, **b** — in the plane located in the middle between both focuses, **c** — in the plane of the focus of external rays F_e

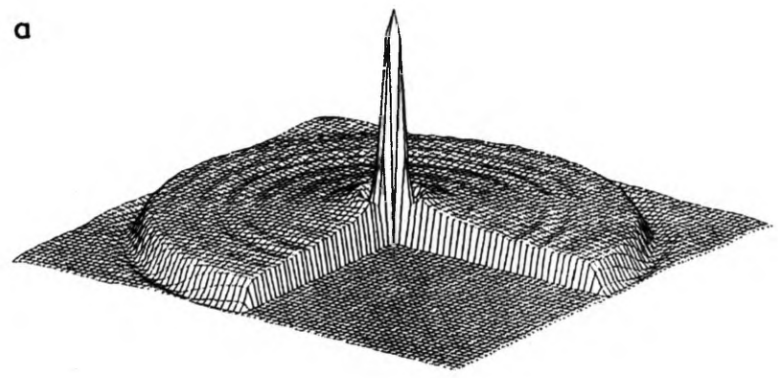

Fig. 5a

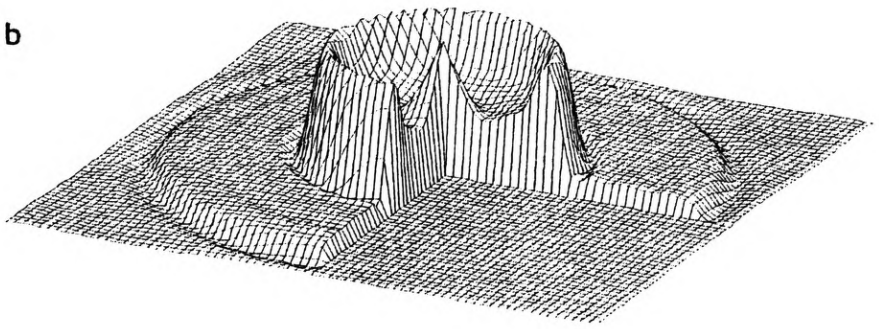

Fig. 5b

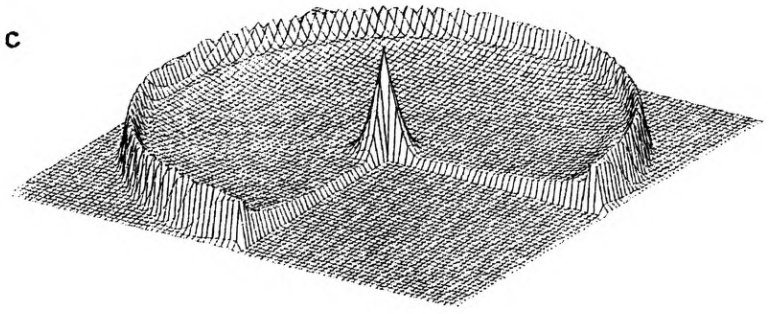

Fig. 5c

Fig. 5. 3-D presentations of the light intensity distribution calculated from spot diagrams given in Fig. 4

distribution I_{foc} was calculated in different planes, located between the paraxial focus and the focus of the most external rays.

3. Results

A problem of the corneal thickness and its distribution over the cornea plays a very important role in the corneal measurement and its diagnosis [12]. Moreover, one expects that the position of the focal region on the axis of the cornea and the light intensity distribution in this region depends on variations of the corneal thickness. We calculated the corneal thickness distribution for different types of approximation of both the corneal surfaces. Figure 6 shows the corneal thickness *vs.* the distance from its axis for four models, approximated by circular, elliptic, parabolic and hyperbolic cosine profiles of both surfaces. In the case of the ellipse the eccentricity of both profiles was equal to $\varepsilon_1 = \varepsilon_2 = 0.75$, close to the ratio of refractive indexes of the air and the aqueous humor (condition for the stigmatic focusing). In the case of hyperbolic cosine profiles, both parameters p_1 and p_2 were equal to 1. As it can be seen from the figure, the form of the curves resembles the real thickness distribution of the human cornea [12].

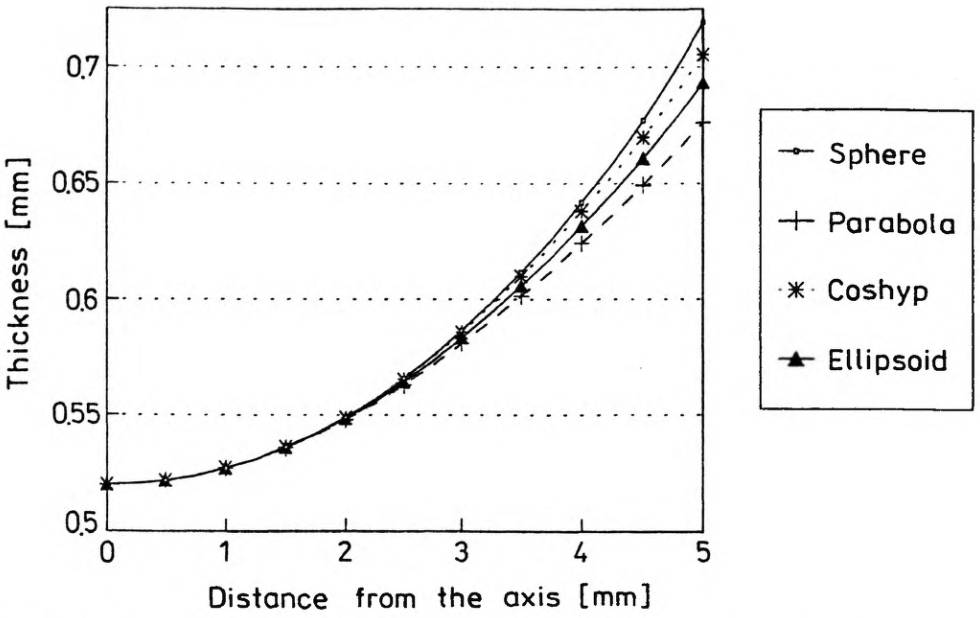

Fig. 6. Corneal thickness *vs.* the distance from the axis for four corneas approximated by circular, elliptic, parabolic and hyperbolic cosine profiles of both surfaces. The eccentricity of both elliptic profiles was equal to $\varepsilon_1 = \varepsilon_2 = 0.75$. Both parameters p_1 and p_2 of hyperbolic cosine profiles were equal to 1

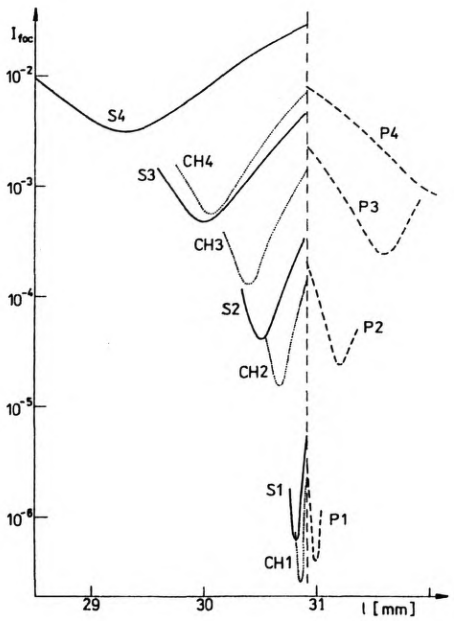

Fig. 7. Graphs of polar moments of the second order I_{foc} of the light intensity distribution, in planes located between focuses F_p and F_{ap} calculated for three models of the cornea. S — sphere, CH — hyperbolic cosine, P — parabola

Results of calculations of the moment I_{foc} for three types of approximation of the corneal topography are given in Fig. 7 (S – sphere, CH – hyperbolic cosine, P – parabola). The respective numbers from 1 to 4 denote values h of the radii (in mm) of the entrance pupil. In the case of hyperbolic cosine profile both parameters p_1 and p_2 were assumed to be equal to 1. The vertical broken line describes the position of the focal plane of paraxial rays. As it can be seen from the figure, the plane of the maximal concentration of the light energy in the focal region shifts differently for the different approximations and for the different diameter of the radius h. For three presented approximations, the concentration of the light intensity for the same entrance pupil is the highest for the hyperbolic cosine profile. In the case of elliptical approximation with eccentricities close to 0.75, curves describing the moment I_{foc} are much below curves presented in the figure for the respective diameter of the pupil. They are concentrated close to the vertical line. For the hyperbolic approximation the respective curves are located more to the right and higher than these for the parabolic approximation.

To investigate the influence of the corneal thickness distribution on the refractive properties of the cornea, values of I_{foc} were computed for the reduced cornea. In this case, the cornea was assumed to be infinitely thin, thus being represented by a single refractive surface. Calculations carried out for the reduced corneas, approximated with the conic curves and the hyperbolic cosine show that the light intensity distribution in their focal region is almost the same as for the corneas approximated by two surfaces of the same type with the thickness distribution similar to those given in Fig. 6. The only difference is that the focal region of these corneas shifts towards the corneal apex in comparison to the corneas with the variable thickness. Differences of moments I_{foc} in the respective planes for both types of corneas are smaller than 1% for four approximations, presented in Fig. 6. To illustrate this effect, the values of I_{foc} computed for both types of the corneal model (single

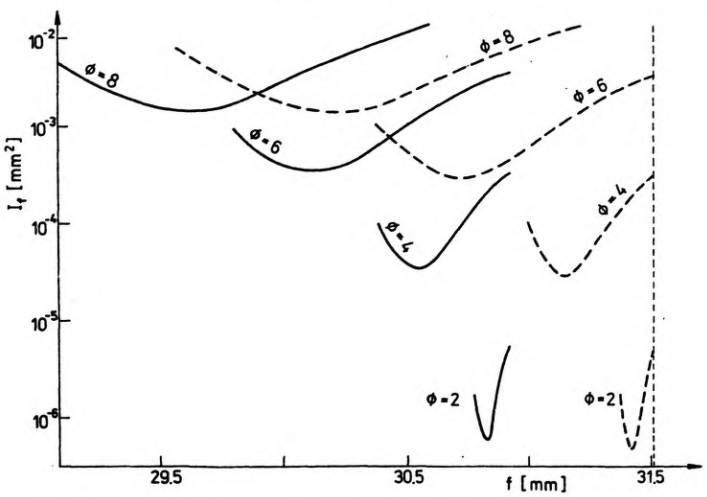

Fig. 8. Graphs of I_{foc} computed for the spherical model of the cornea, with a single (continuous line) and double (broken line) refractive surfaces

refractive surface and the cornea with a variable thickness) for the spherical approximation are presented in Fig. 8. As it can be noticed from the figure, forms and the values of respective curves, calculated for different diameters of the entrance pupil are almost the same but they are shifted horizontally with respect to each other. Figure 9 shows the optical power of the corneal model, for the reduced spherical and the double spherical ($R_{01} = 7.8$ mm, $R_{02} = 6.5$ mm and $d = 0.52$ mm) approximations *vs.* the radius of the entrance pupil, calculated for the respective minimal value of I_{foc}. It can be noticed that the difference between both curves amounts to about 0.75 D. The shift of the respective optical power during increase of the pupil diameter from 2 to 8 mm is equal to about 1.65 D.

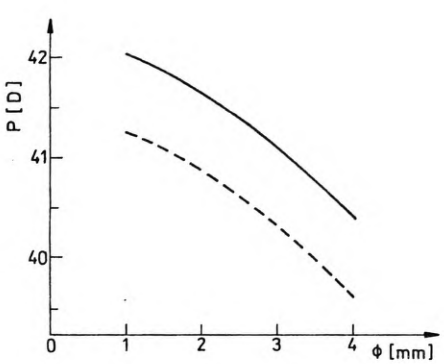

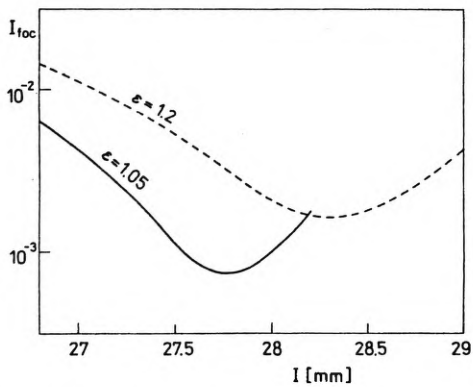

Fig. 9. Optical power of the cornea, calculated for the single spherical approximation (continuous line) and for two spherical surfaces (broken line), $R_{01} = 7.8$ mm, $R_{02} = 6.5$ mm and $d = 0.52$ mm, referred to the respective minimal value of I_{foc}

Fig. 10. Distribution of I_{foc} *vs.* the position on the corneal axis for two hyperbolic approximations (case of keratoconus), with the eccentricity $\varepsilon = 1.05$ and $\varepsilon = 1.2$ for the radius of the entrance pupil $h = 3$ mm

To calculate the refractive properties of keratoconic cornea, the corneal model was approximated by use of hyperbola [13] with the central radius of curvature R_0 equal to 6.75 mm and eccentricities amounted to $\varepsilon = 1.05$ or $\varepsilon = 1.2$, respectively. Figure 10 presents the distribution of I_{foc} for both hyperbolic approximations and for the radius of the entrance pupil $h = 3$ mm. By comparing these curves with those having the same diameter of the entrance pupil and given in Fig. 7, it can be noticed that values of I_{foc} for the hyperbolic approximations are significantly higher. Thus, the light intensity concentration in the focal area is the highest in this case, in spite of the smallest value of the focal distance.

4. Discussion

According to our calculations the form of the function approximating the corneal contour influences significantly he refractive properties of the corneal model. Although we exploited only the ray tracing method without taking account of any diffraction effects, the obtained results represent the corneal refractivity with a good

accuracy. The asphericity of the corneal contour significantly reduces the spherical aberrations of the cornea. If the corneal contour can be approximated by an ellipse with an eccentricity $\varepsilon \approx 0.75$, close to the inverse of the refractive index of the aqueous humor (1.3374), its spherical aberration can be practically neglected [11]. However, KIELY *et al.* [8] have shown on 176 healthy eyes that the mean value of the eccentricity of elliptic approximation was 0.51 with a standard deviation 0.42. So, the spherical aberration of the cornea is not corrected completely in a population. The calculation performed in this work showed that the corneal thickness increasing monotonically from about 0.5 mm at the apex to about 0.7 mm close to the limbus does not influence essentially its shperical aberration and the distribution of the light intensity in the focal region of the cornea. This causes, however, the shift of its focal region by about 0.7 mm apart from the apex and, finally, the respective reduction of the optical power.

It should be remembered that the cornea plays different roles (chemical, physiological, *etc.*) being among other both a lens but also as a complex, aspheric biomechanical shell, the latter limiting the anterior chamber of the eye and protects the eye from mechanical injuries. Thus, the refractive quality of the cornea is indissolubly connected with its biomechanical properties. The corneal geometry fulfils conditions of reduction of optical aberrations, and partially conditions of an optimal biomechanical shell. Since sizes of spot diagrams of the cornea calculated in the paper are significantly greater than those observed on the retina, the eye lens has to assure the increase of the optical power of the eye and correct the rest of axial optical aberrations.

References

[1] LE GRAND Y., EL HAGE S. G., *Physiological Optics*, Springer Series in Optical Series, Vol. 13, [Ed.] D. L. MacAdam, Springer-Verlag, Berlin 1980.
[2] LOTMAR W., J. Opt. Soc. Am. **61** (1971), 1522.
[3] MALONEY R. K., BOGAN S. J., WARING G. O., III, Am. J. Ophthalmology **115** (1993), 31.
[4] CAMP J. J., MAGUIRE L. J., CAMERON B. M., ROBB R. A., Am. J. Ophthalmology **109** (1990), 379.
[5] SEILER T., RECKMANN W., MALONEY R. K., J. Cataract. Refr. Surg. **19** (Suppl.), (1993), 155.
[6] WILSON S. E., KLYCE S. D., Arch. Ophthalmol. **109** (1991), 349.
[7] BONNET R., COCHET P., Am. J. Optom. **39** (1962), 227.
[8] KIELY P. M., SMITH G. M., CARNEY L. G., Opt. Acta **29** (1982), 1027.
[9] GUILLON M., LYDON D. P. M., WILSON C., Ophthal. Physiol. Opt. **6** (1986), 47.
[10] EDMUND C., Am. J. Optom. Physiol. Optics **64** (1987), 846.
[11] KASPRZAK H., JANKOWSKA-KUCHTA E., *New analytical approximation of the corneal topography*, J. Modern Opt., in press.
[12] EDMUND C., Acta Ophthalm. **65** (1987), 147.
[13] MANDELL R. B., POLSE K. A., Arch. Ophthalmol. **82** (1969), 182.

Received October 23, 1995